



Bose-Einstein correlations in W-pair decays with an event-mixing technique

S. Schael, R. Barate, R. Brunelière, I. De Bonis, D. Décamp, C. Goy, S. Jézéquel, J.P. Lees, F. Martin, E. Merle, et al.

► To cite this version:

S. Schael, R. Barate, R. Brunelière, I. De Bonis, D. Décamp, et al.. Bose-Einstein correlations in W-pair decays with an event-mixing technique. *Physics Letters B*, Elsevier, 2005, 606, pp.265-275. <10.1016/j.physletb.2004.12.018>. <in2p3-00023313>

HAL Id: in2p3-00023313

<http://hal.in2p3.fr/in2p3-00023313>

Submitted on 16 Nov 2004

HAL is a multi-disciplinary open access archive for the deposit and dissemination of scientific research documents, whether they are published or not. The documents may come from teaching and research institutions in France or abroad, or from public or private research centers.

L'archive ouverte pluridisciplinaire **HAL**, est destinée au dépôt et à la diffusion de documents scientifiques de niveau recherche, publiés ou non, émanant des établissements d'enseignement et de recherche français ou étrangers, des laboratoires publics ou privés.

Bose-Einstein correlations in W -pair decays with an event-mixing technique

The ALEPH Collaboration ^{*)}

Abstract

Bose-Einstein correlations in W -pair decays are studied using data collected by the ALEPH detector at LEP at e^+e^- centre-of-mass energies from 183 to 209 GeV. The analysis is based on the comparison of $WW \rightarrow q\bar{q}q\bar{q}$ events to “mixed” events constructed with the hadronic part of $WW \rightarrow q\bar{q}\ell\nu$ events. The data are in agreement with the hypothesis that Bose-Einstein correlations are present only for pions from the same W decay. The JETSET model with Bose-Einstein correlations between pions from different W bosons is disfavoured.

submitted to Physics Letters B

^{*)} see next page for the list of authors

The ALEPH Collaboration

S. Schael

Physikalisches Institut der RWTH-Aachen, D-52056 Aachen, Germany

R. Barate, R. Brunelière, I. De Bonis, D. Decamp, C. Goy, S. Jézéquel, J.-P. Lees, F. Martin, E. Merle, M.-N. Minard, B. Pietrzyk, B. Trocmé

Laboratoire de Physique des Particules (LAPP), IN²P³-CNRS, F-74019 Annecy-le-Vieux Cedex, France

S. Bravo, M.P. Casado, M. Chmeissani, J.M. Crespo, E. Fernandez, M. Fernandez-Bosman, Ll. Garrido,¹⁵ M. Martinez, A. Pacheco, H. Ruiz

Institut de Física d'Altes Energies, Universitat Autònoma de Barcelona, E-08193 Bellaterra (Barcelona), Spain⁷

A. Colaleo, D. Creanza, N. De Filippis, M. de Palma, G. Iaselli, G. Maggi, M. Maggi, S. Nuzzo, A. Ranieri, G. Raso,²⁴ F. Ruggieri, G. Selvaggi, L. Silvestris, P. Tempesta, A. Tricomi,³ G. Zito

Dipartimento di Fisica, INFN Sezione di Bari, I-70126 Bari, Italy

X. Huang, J. Lin, Q. Ouyang, T. Wang, Y. Xie, R. Xu, S. Xue, J. Zhang, L. Zhang, W. Zhao

Institute of High Energy Physics, Academia Sinica, Beijing, The People's Republic of China⁸

D. Abbaneo, T. Barklow,²⁶ O. Buchmüller,²⁶ M. Cattaneo, B. Clerbaux,²³ H. Drevermann, R.W. Forty, M. Frank, F. Gianotti, J.B. Hansen, J. Harvey, D.E. Hutchcroft,³⁰ P. Janot, B. Jost, M. Kado,² P. Mato, A. Moutoussi, F. Ranjard, L. Rolandi, D. Schlatter, G. Sguazzoni, F. Teubert, A. Valassi, I. Videau

European Laboratory for Particle Physics (CERN), CH-1211 Geneva 23, Switzerland

F. Badaud, S. Dessagne, A. Falvard,²⁰ D. Fayolle, P. Gay, J. Jousset, B. Michel, S. Monteil, D. Pallin, J.M. Pascolo, P. Perret

Laboratoire de Physique Corpusculaire, Université Blaise Pascal, IN²P³-CNRS, Clermont-Ferrand, F-63177 Aubière, France

J.D. Hansen, J.R. Hansen, P.H. Hansen, A.C. Kraan, B.S. Nilsson

Niels Bohr Institute, 2100 Copenhagen, DK-Denmark⁹

A. Kyriakis, C. Markou, E. Simopoulou, A. Vayaki, K. Zachariadou

Nuclear Research Center Demokritos (NRCD), GR-15310 Attiki, Greece

A. Blondel,¹² J.-C. Brient, F. Machefert, A. Rougé, H. Videau

Laboratoire Leprince-Ringuet, Ecole Polytechnique, IN²P³-CNRS, F-91128 Palaiseau Cedex, France

V. Ciulli, E. Focardi, G. Parrini

Dipartimento di Fisica, Università di Firenze, INFN Sezione di Firenze, I-50125 Firenze, Italy

A. Antonelli, M. Antonelli, G. Bencivenni, F. Bossi, G. Capon, F. Cerutti, V. Chiarella, P. Laurelli, G. Mannocchi,⁵ G.P. Murtas, L. Passalacqua

Laboratori Nazionali dell'INFN (LNF-INFN), I-00044 Frascati, Italy

J. Kennedy, J.G. Lynch, P. Negus, V. O'Shea, A.S. Thompson

Department of Physics and Astronomy, University of Glasgow, Glasgow G12 8QQ, United Kingdom¹⁰

S. Wasserbaech

Utah Valley State College, Orem, UT 84058, U.S.A.

R. Cavanaugh,⁴ S. Dhamotharan,²¹ C. Geweniger, P. Hanke, V. Hepp, E.E. Kluge, A. Putzer, H. Stenzel, K. Tittel, M. Wunsch¹⁹

Kirchhoff-Institut für Physik, Universität Heidelberg, D-69120 Heidelberg, Germany¹⁶

R. Beuselinck, W. Cameron, G. Davies, P.J. Dornan, M. Girone,¹ N. Marinelli, J. Nowell, S.A. Rutherford, J.K. Sedgbeer, J.C. Thompson,¹⁴ R. White

*Department of Physics, Imperial College, London SW7 2BZ, United Kingdom*¹⁰

V.M. Ghete, P. Girtler, E. Kneringer, D. Kuhn, G. Rudolph

*Institut für Experimentalphysik, Universität Innsbruck, A-6020 Innsbruck, Austria*¹⁸

E. Bouhova-Thacker, C.K. Bowdery, D.P. Clarke, G. Ellis, A.J. Finch, F. Foster, G. Hughes, R.W.L. Jones, M.R. Pearson, N.A. Robertson, M. Smizanska

*Department of Physics, University of Lancaster, Lancaster LA1 4YB, United Kingdom*¹⁰

O. van der Aa, C. Delaere,²⁸ G. Leibenguth,³¹ V. Lemaitre²⁹

Institut de Physique Nucléaire, Département de Physique, Université Catholique de Louvain, 1348 Louvain-la-Neuve, Belgium

U. Blumenschein, F. Hölldorfer, K. Jakobs, F. Kayser, K. Kleinknecht, A.-S. Müller, B. Renk, H.-G. Sander, S. Schmeling, H. Wachsmuth, C. Zeitnitz, T. Ziegler

*Institut für Physik, Universität Mainz, D-55099 Mainz, Germany*¹⁶

A. Bonissent, P. Coyle, C. Curtil, A. Ealet, D. Fouchez, P. Payre, A. Tilquin

Centre de Physique des Particules de Marseille, Univ Méditerranée, IN²P³-CNRS, F-13288 Marseille, France

F. Ragusa

Dipartimento di Fisica, Università di Milano e INFN Sezione di Milano, I-20133 Milano, Italy.

A. David, H. Dietl,³² G. Ganis,²⁷ K. Hüttmann, G. Lütjens, W. Männer³², H.-G. Moser, R. Settles, M. Villegas, G. Wolf

*Max-Planck-Institut für Physik, Werner-Heisenberg-Institut, D-80805 München, Germany*¹⁶

J. Boucrot, O. Callot, M. Davier, L. Duflot, J.-F. Grivaz, Ph. Heusse, A. Jacholkowska,⁶ L. Serin, J.-J. Veillet

Laboratoire de l'Accélérateur Linéaire, Université de Paris-Sud, IN²P³-CNRS, F-91898 Orsay Cedex, France

P. Azzurri, G. Bagliesi, T. Boccali, L. Foà, A. Giammanco, A. Giassi, F. Ligabue, A. Messineo, F. Palla, G. Sanguinetti, A. Sciabà, P. Spagnolo, R. Tenchini, A. Venturi, P.G. Verдини

Dipartimento di Fisica dell'Università, INFN Sezione di Pisa, e Scuola Normale Superiore, I-56010 Pisa, Italy

O. Awunor, G.A. Blair, G. Cowan, A. Garcia-Bellido, M.G. Green, T. Medcalf, A. Misiejuk, J.A. Strong, P. Teixeira-Dias

*Department of Physics, Royal Holloway & Bedford New College, University of London, Egham, Surrey TW20 OEX, United Kingdom*¹⁰

R.W. Clift, T.R. Edgecock, P.R. Norton, I.R. Tomalin, J.J. Ward

*Particle Physics Dept., Rutherford Appleton Laboratory, Chilton, Didcot, Oxon OX11 0QX, United Kingdom*¹⁰

B. Bloch-Devaux, D. Boumediene, P. Colas, B. Fabbro, E. Lançon, M.-C. Lemaire, E. Locci, P. Perez, J. Rander, B. Tuchming, B. Vallage

*CEA, DAPNIA/Service de Physique des Particules, CE-Saclay, F-91191 Gif-sur-Yvette Cedex, France*¹⁷

A.M. Litke, G. Taylor

*Institute for Particle Physics, University of California at Santa Cruz, Santa Cruz, CA 95064, USA*²²

C.N. Booth, S. Cartwright, F. Combley,²⁵ P.N. Hodgson, M. Lehto, L.F. Thompson

*Department of Physics, University of Sheffield, Sheffield S3 7RH, United Kingdom*¹⁰

A. Böhrer, S. Brandt, C. Grupen, J. Hess, A. Ngac, G. Prange

*Fachbereich Physik, Universität Siegen, D-57068 Siegen, Germany*¹⁶

C. Borean, G. Giannini

Dipartimento di Fisica, Università di Trieste e INFN Sezione di Trieste, I-34127 Trieste, Italy

H. He, J. Putz, J. Rothberg

Experimental Elementary Particle Physics, University of Washington, Seattle, WA 98195 U.S.A.

S.R. Armstrong, K. Berkelman, K. Cranmer, D.P.S. Ferguson, Y. Gao,¹³ S. González, O.J. Hayes, H. Hu, S. Jin, J. Kile, P.A. McNamara III, J. Nielsen, Y.B. Pan, J.H. von Wimmersperg-Toeller, W. Wiedenmann, J. Wu, Sau Lan Wu, X. Wu, G. Zobernig

*Department of Physics, University of Wisconsin, Madison, WI 53706, USA*¹¹

G. Dissertori

Institute for Particle Physics, ETH Hönggerberg, 8093 Zürich, Switzerland.

¹Also at CERN, 1211 Geneva 23, Switzerland.

²Now at Fermilab, PO Box 500, MS 352, Batavia, IL 60510, USA

³Also at Dipartimento di Fisica di Catania and INFN Sezione di Catania, 95129 Catania, Italy.

⁴Now at University of Florida, Department of Physics, Gainesville, Florida 32611-8440, USA

⁵Also IFSI sezione di Torino, CNR, Italy.

⁶Also at Groupe d'Astroparticules de Montpellier, Université de Montpellier II, 34095, Montpellier, France.

⁷Supported by CICYT, Spain.

⁸Supported by the National Science Foundation of China.

⁹Supported by the Danish Natural Science Research Council.

¹⁰Supported by the UK Particle Physics and Astronomy Research Council.

¹¹Supported by the US Department of Energy, grant DE-FG0295-ER40896.

¹²Now at Departement de Physique Corpusculaire, Université de Genève, 1211 Genève 4, Switzerland.

¹³Also at Department of Physics, Tsinghua University, Beijing, The People's Republic of China.

¹⁴Supported by the Leverhulme Trust.

¹⁵Permanent address: Universitat de Barcelona, 08208 Barcelona, Spain.

¹⁶Supported by Bundesministerium für Bildung und Forschung, Germany.

¹⁷Supported by the Direction des Sciences de la Matière, C.E.A.

¹⁸Supported by the Austrian Ministry for Science and Transport.

¹⁹Now at SAP AG, 69185 Walldorf, Germany

²⁰Now at Groupe d'Astroparticules de Montpellier, Université de Montpellier II, 34095 Montpellier, France.

²¹Now at BNP Paribas, 60325 Frankfurt am Main, Germany

²²Supported by the US Department of Energy, grant DE-FG03-92ER40689.

²³Now at Institut Inter-universitaire des hautes Energies (IHE), CP 230, Université Libre de Bruxelles, 1050 Bruxelles, Belgique

²⁴Now at Dipartimento di Fisica e Tecnologia Relative, Università di Palermo, Palermo, Italy.

²⁵Deceased.

²⁶Now at SLAC, Stanford, CA 94309, U.S.A

²⁷Now at CERN, 1211 Geneva 23, Switzerland

²⁸Research Fellow of the Belgium FNRS

²⁹Research Associate of the Belgium FNRS

³⁰Now at Liverpool University, Liverpool L69 7ZE, United Kingdom

³¹Supported by the Federal Office for Scientific, Technical and Cultural Affairs through the Interuniversity Attraction Pole P5/27

³²Now at Henryk Niewodniczski Institute of Nuclear Physics, Polish Academy of Sciences, Cracow, Poland

1 Introduction

The existence of Bose-Einstein (BE) correlations between identical bosons in hadronic final states is well established. This effect was first observed experimentally in like-sign charged pions produced in $p\bar{p}$ collisions [1] and then in different hadronic final states produced by various initial states [2–8]. It leads to an enhancement of the two-particle differential cross section for pairs of identical pions close in phase space. More recently BE correlations were also studied in hadronic Z decays [9–12], and observations of these correlations in W-pair production at LEP 2 have already been reported [13–16]. Theoretically, it is unclear to what extent Bose-Einstein interference occurs between the decay products of the two W bosons in the $WW \rightarrow q\bar{q}q\bar{q}$ channel [17]. Such interference, if sizeable, may influence the W mass measurement [17, 18].

The ALEPH analysis of BE correlations in W-pair decays based on the comparison of like-sign and unlike-sign pion pairs is described in detail in Ref. [13]. In view of a sound comparison and combination with other LEP experiments the analysis presented here uses the so-called “mixed” method [19]. In this method fully hadronic W-pair decays are compared with a reference event sample constructed by mixing the hadronic parts of semileptonic decays, $WW \rightarrow q\bar{q}\ell\nu$. By construction, these “mixed” events have BE correlations between pions from the decay of the same W, but none between pions from different W bosons. The comparison is therefore sensitive to the Bose-Einstein enhancement at low momentum transfer, Q , of the two-particle differential cross section for like-sign pions from different W bosons in $WW \rightarrow q\bar{q}q\bar{q}$ events. The variable Q is defined as

$$Q = \sqrt{-(p_1 - p_2)^2}, \quad (1)$$

in which p_1 and p_2 are the four-momenta of the two pions.

2 The ALEPH detector

A detailed description of the ALEPH detector can be found in Ref. [20], and of its performance in Ref. [21]. Charged particles are detected in the central part, consisting of a precision silicon vertex detector, a cylindrical drift chamber and a large time projection chamber, measuring altogether up to 31 space points along the charged particle trajectories. A 1.5 T axial magnetic field is provided by a superconducting solenoidal coil. Charged particle transverse momenta are reconstructed with a $1/p_T$ resolution of $(6 \times 10^{-4} \oplus 5 \times 10^{-3}/p_T) (\text{GeV}/c)^{-1}$. In the following, *good* tracks are defined as charged particle tracks reconstructed with at least four hits in the time projection chamber, originating from within a cylinder of length 20 cm and radius 2 cm coaxial with the beam and centred at the nominal collision point, and with a polar angle θ with respect to the beam such that $|\cos \theta| < 0.95$.

Jets originating from b quarks are identified with a lifetime b-tagging algorithm [22], which takes advantage of the three-dimensional impact parameter resolution of charged particle tracks. For tracks with two space points in the silicon vertex detector (*i.e.*, $|\cos \theta| < 0.7$), this resolution can be parametrized as $(25 + 95/p) \mu\text{m}$, with the momentum p in GeV/c .

In addition to its rôle as a tracking device, the time projection chamber also measures the specific energy loss by ionization dE/dx . It allows low momentum electrons up to 8 GeV/c to

be separated from other charged particle species by more than three standard deviations.

Electrons (and photons) are also identified by the characteristic longitudinal and transverse developments of the associated showers in the electromagnetic calorimeter, a 22 radiation length thick sandwich of lead planes and proportional wire chambers with fine read-out segmentation. The relative energy resolution achieved is $0.18/\sqrt{E}$ (E in GeV) for isolated electrons and photons.

Photon conversions to e^+e^- in the detector material are identified as a pair of oppositely-charged particle tracks satisfying the following conditions: *(i)* the measured dE/dx of the two tracks is within 3σ of that expected for electrons; *(ii)* the distance between the two tracks at their point of closest approach is smaller than 1 cm in the plane transverse to the beam and less than 2 cm along the beam direction; and *(iii)* the invariant mass is smaller than $30 \text{ MeV}/c^2$, when calculated as for an e^+e^- pair coming from this point of closest approach.

Muons are identified by their characteristic penetration pattern in the hadron calorimeter, a 1.5 m thick iron yoke interleaved with 23 layers of streamer tubes, together with two surrounding double-layers of muon chambers. In association with the electromagnetic calorimeter, the hadron calorimeter also provides a measurement of the hadronic energy with a relative resolution of $0.85/\sqrt{E}$ (E in GeV).

The total visible energy is measured with an energy-flow reconstruction algorithm which combines all the above measurements, supplemented by the energy detected at low polar angle (down to 24 mrad from the beam axis) by two additional electromagnetic calorimeters, used for the luminosity determination. In addition to the total visible-energy measurement, the energy-flow reconstruction algorithm also provides a list of reconstructed objects, classified as charged particles, photons and neutral hadrons, and called *energy-flow particles* in the following.

3 Data samples, event and track selection

The results presented in this letter have been obtained with data collected by the ALEPH detector at centre-of-mass energies between 183 and 209 GeV. The event selections are those used in Ref. [23] with an additional cut (0.3) on the neural-network selection function for $WW \rightarrow q\bar{q}q\bar{q}$ events. The integrated luminosity used in this analysis is 683 pb^{-1} , the number of events selected in the $WW \rightarrow q\bar{q}q\bar{q}$ channel is 6155 and it is 4849 in the $WW \rightarrow q\bar{q}\ell\nu$ channel.

Only good tracks are considered as possible pion candidates, but those identified as electrons and muons in the calorimeters, and those identified as arising from a photon conversion, or K^0 and Λ^0 decay, are rejected. In addition, good tracks with a momentum smaller than $5 \text{ GeV}/c$ and with a dE/dx compatible with that of an electron within three standard deviations are excluded from the data sample.

Successive arcs of spiraling tracks passing near the time projection chamber membrane are sometimes split into multiple tracks very close in momentum and in space. To reject them, tracks are required to have at least three hits in the first five layers of the time projection chamber, which in cases where a single particle is incorrectly reconstructed as two or more separate tracks, virtually eliminates the possibility of more than one of these tracks being accepted.

Finally, potential problems of pattern recognition with close tracks are alleviated by only considering pairs of tracks with an opening angle in excess of 3° .

After this selection Monte Carlo studies show that the purity of the $\pi\pi$ pairs is about 80% in the low Q region where BE correlations are expected.

4 Description of the event mixing technique

Mixed events are constructed from the hadronic parts of two different $WW \rightarrow q\bar{q}\ell\nu$ events, taking into account the electric charge of the leptonically decaying W boson so that a W^+ is always mixed with a W^- . The electric charge of τ decays is determined as explained in Ref. [24]. Each semileptonic event is used at most once in this analysis. Pairs of selected semileptonic events are chosen at random, until there are no remaining semileptonic events with leptonically decaying W bosons of a given charge. In total 2406 such events are constructed.

Momentum conservation is imposed on mixed events as follows: all reconstructed particles of one of the two W bosons, chosen at random, are first boosted to the rest frame of this W boson, and then boosted again to have a momentum of the first W boson exactly opposite to that of the second W boson.

5 Monte Carlo simulation

Bose-Einstein correlations among identical bosons in multihadronic final states are simulated with the JETSET model (option BE₃₂ with Gaussian parametrization [25] implemented in the PYTHIA Monte Carlo generator [26], version 6.1). A global fit of the free BE and QCD parameters of the model is performed using hadronic Z decay data.

The variable parameters considered are the strength parameter $\lambda_{\text{BE}}^{\text{input}}$ and the width parameter $\sigma_{\text{BE}}^{\text{input}}$. The latter can be interpreted as the inverse size of the pion emission region. The minimum width of resonances for which the decay products are assumed to take part in the BE correlation effect is kept at its default value (0.020 GeV). As the JETSET method consists of shifting momenta of identical bosons close in phase space, the jet properties are changed and a simultaneous tuning of the most important fragmentation parameters becomes necessary. The JETSET parameters Λ_{QCD} , Q_0 , σ , a and b are considered in this global tuning. The set of distributions includes the normalized Q -distribution of same-sign charged particle pairs, in the range 0.04 – 1.0 GeV, together with several event-shape and inclusive charged particle momentum distributions. The tuning procedure is described in Ref. [27]. The distributions are measured in $Z \rightarrow q\bar{q}$ events with natural flavour mix and in a sub-sample depleted in $b\bar{b}$.

Standard cuts [27] are applied to select 10^6 hadronic Z decays recorded in the 1994 data taking period. By requiring the probability P_{uds} [22] that all tracks originate from the main interaction vertex to be larger than $10^{-2.2}$, the $b\bar{b}$ content is reduced to 5%.

To correct the data for the effects of the detector and of the selection cuts, bin-by-bin correction factors determined by Monte Carlo simulation are applied. It is found that at small

Table 1: Fitted BE correlation and QCD parameters for $Z \rightarrow$ all flavours and for light flavours (udsc). Since the parameters a and b are strongly correlated, one of them, b , is held fixed for technical reasons. The parameter ϵ_b is adjusted to the measured b-quark fragmentation function [28]. The PYTHIA6.1 version used includes ALEPH-specific modifications to heavy flavour decay tables. The Q -distribution is not used in the no-BE correlation (noBEC) fits.

parameter	PARJ	all flavours		udsc	
		BEC	noBEC	BEC	noBEC
$\lambda_{\text{BE}}^{\text{input}}$	(92)	1.107	-	1.137	-
$\sigma_{\text{BE}}^{\text{input}}$ (GeV)	(93)	0.330	-	0.335	-
Λ_{QCD} (GeV)	(81)	0.274	0.269	0.276	0.269
Q_0 (GeV)	(82)	1.67	1.43	1.76	1.44
σ (GeV)	(21)	0.379	0.369	0.375	0.364
a	(41)	0.502	0.506	0.509	0.508
b (GeV $^{-2}$)	(42)	0.800	0.900	0.800	0.900
ϵ_b	(55)	-0.0020	-0.0024	-0.0020	-0.0024

values of Q , below 0.3 GeV, the correction factors depend on the BE correlation parameters. A three-step iterative procedure is therefore applied. The corrected Q -distribution for the b-depleted case is shown in Fig. 1.

The best fit is shown as solid line in Fig. 1. It provides a reasonably good description of the data. The maximum deviation is 4% for Q below 0.1 GeV. The PYTHIA simulation without BE correlations does not describe the data. The distribution of opposite-sign charged particle pairs, if restricted to Q values below the K_S^0 and resonance regions, is also well described but has negligible effect on the results if included in the fit. The fitted parameters are given in Table 1. The correlation coefficient between $\lambda_{\text{BE}}^{\text{input}}$ and $\sigma_{\text{BE}}^{\text{input}}$ is large and amounts to -0.79 . The values obtained from the b-depleted sample (“udsc”) are used for the simulation of BE effects in W decays in the following. The values obtained from the “all flavours” fit are used for the simulation of the $q\bar{q}$ event sample with BE correlations needed for the background subtraction.

For the study of W decays two Monte Carlo simulations are performed. The “BEI” (Bose-Einstein Inside) stands for the case in which BE correlations do not occur between decay products of different W bosons, and “BEB” (Bose-Einstein Both) if they do. The programs KORALW [29] and KKMC [30] are used to generate WW and $q\bar{q}$ events, respectively. The simulated distributions for this analysis are the sum of distributions generated at different centre-of-mass energies weighted by the integrated luminosities.

6 Analysis method

The Bose-Einstein enhancement in pair production of identical pions is studied using a two-particle correlation function, derived from the ratio of the number of like-sign pion pairs in events selected as $WW \rightarrow q\bar{q}q\bar{q}$ decays ($N_{\text{Sel. } 4q}^{++,-,-}$) to the number of like-sign pion pairs in mixed events ($N_{\text{Mixed}}^{++,-,-}$). Since the event mixing technique could introduce systematic distortions to the distribution of this variable, the ratio for data is divided by the same ratio obtained from

the WW events Monte Carlo simulation with BEI correlations. The resulting double ratio is given by

$$D'(Q) = \frac{\left(N_{\text{Sel. } 4q}^{++,--} / N_{\text{Mixed}}^{++,--}\right)^{\text{data}}}{\left(N_{\text{Sel. } 4q}^{++,--} / N_{\text{Mixed}}^{++,--}\right)^{\text{MC,BEI}}} . \quad (2)$$

The $q\bar{q}$ background is subtracted from the data selected as $WW \rightarrow q\bar{q}q\bar{q}$ decays using events generated with the parameters given in Table 1. Any significant deviation from unity of the measured $D'(Q)$ at low Q would indicate BE correlations between pions from different W bosons. The same formula is used with the numerator computed from Monte Carlo simulations where BE correlations in the WW signal are simulated according to the BEB model. This allows the measured $D'(Q)$ distribution at low Q to be compared with the prediction of the BEB Monte Carlo simulation, thus providing evidence for or against the validity of the BEB model.

An alternative distribution is obtained from the difference of the number of like-sign pion pairs in events selected as $WW \rightarrow q\bar{q}q\bar{q}$ decays and the number of like-sign pion pairs in mixed events in both data and WW events Monte Carlo simulation,

$$\Delta\rho'(Q) = \left(N_{\text{Sel. } 4q}^{++,--} - N_{\text{Mixed}}^{++,--}\right)^{\text{data}} - \left(N_{\text{Sel. } 4q}^{++,--} - N_{\text{Mixed}}^{++,--}\right)^{\text{MC,BEI}} . \quad (3)$$

A deviation of $\Delta\rho'(Q)$ from zero at low Q would also indicate the existence of BE correlations between pions originating from different W bosons.

7 Results

The data and simulated BEB distributions of $D'(Q)$ are shown in Fig. 2. They are fitted, in the Q range 0-3 GeV, with the following functional form:

$$D'(Q) = \kappa(1 + \lambda e^{-\sigma^2 Q^2}) . \quad (4)$$

The parameters λ and σ describe BE correlations, while the variable κ gives the overall normalization. The fitted values should not be compared directly to those obtained in Ref. [13], that were used to parametrize the distribution of a different variable (R^*). The variables λ and σ used here can be compared, however, to the variables Λ and k used by L3 [16], while they are different from the variables Λ and R used by the OPAL [15] Collaboration because of different fitting formulae.

The results are given in Table 2. The simulated BEB distribution is fitted with three parameters. The data distribution does not show any enhancement in the region where BE correlations are expected. Therefore data are fitted with the value of σ fixed to that obtained from a fit to the BEB distribution. In contrast to the analysis in Ref. [13], the bin-to-bin correlations are important. In order to avoid biases from statistical fluctuations the expected uncertainties are used in the fit.

The alternative $\Delta\rho'(Q)$ distribution is shown in Fig. 3. The data and simulated BEB distributions are integrated to $Q_{\text{max}} = 0.6$ GeV. The value of the integral ($I_{\Delta\rho'}$) is -0.127 ± 0.143 for the data and 0.699 ± 0.055 for the BEB simulation.

The lower parts of Figs. 2 and 3 show the corresponding distributions for the unlike-sign pairs. The enhancement of the BEB simulation at low Q is interpreted as a feature of the JETSET implementation of BE correlations.

Table 2: Results of the fit to the $D'(Q)$ distributions for data and simulation. The correlation between λ and σ is denoted $C_{\lambda\sigma}$. Only statistical uncertainties are shown.

Sample	κ	λ	σ (GeV $^{-1}$)	$C_{\lambda\sigma}$
three-parameter fit to $\kappa(1 + \lambda e^{-\sigma^2 Q^2})$				
BEB	0.985 ± 0.003	0.081 ± 0.005	2.31 ± 0.09	0.53
two-parameter fit to $\kappa(1 + \lambda e^{-2.31^2 Q^2})$				
Data	0.993 ± 0.008	-0.004 ± 0.011		
BEB	0.985 ± 0.003	0.081 ± 0.004		

8 Systematic uncertainties

Systematic uncertainties are listed in Table 3. They are divided into four categories and discussed below:

- *Track selection bias.* The double ratio (Eq. 2) and the double difference (Eq. 3) are robust against systematic biases from the track selection. A set of cuts for track selection is used in the analysis as described in Section 3. As a cross-check, the analysis is repeated with these cuts removed one by one in the simulation only. The maximum difference is conservatively given as systematic uncertainty in Table 3.
- *Event selection.* In order to cross-check the quality of the mixing technique, the whole analysis is repeated with different Neural Network cuts for the $WW \rightarrow q\bar{q}q\bar{q}$ selection and different semileptonic selections. The differences to the results of the standard analysis have a large statistical component. Conservatively the maximum difference is given as systematic uncertainty in Table 3.
- *Background subtraction.* The $q\bar{q}$ background is subtracted from the data selected as $WW \rightarrow q\bar{q}q\bar{q}$ decays. It was found that the Monte Carlo simulation with $\lambda_{\text{BE}}^{\text{input}}=0.9$ describes better hadronic Z decays into four jets. The difference between results obtained with the $q\bar{q}$ background subtraction simulated with the parameters given in Table 1 and simulated with the parameter $\lambda_{\text{BE}}^{\text{input}}=0.9$ is treated as systematic uncertainty. Additional uncertainties arise from the 3% uncertainty in the $q\bar{q}$ production cross section and because no background subtraction is performed in mixed events.
- *Close tracks.* The whole analysis is repeated without the 3° opening angle cut. The results are found to be statistically compatible with those obtained with this cut.

Table 3: Systematic uncertainties

	λ	$I_{\Delta\rho'}$
track selection	0.006	0.092
event selection	0.012	0.171
background subtraction	0.003	0.044
total	0.014	0.199

9 Conclusions

Bose-Einstein correlations in W-pair decays have been studied by comparing $WW \rightarrow q\bar{q}q\bar{q}$ events to those constructed by mixing the hadronic parts of two selected $WW \rightarrow q\bar{q}\ell\nu$ decays. When the Bose-Einstein source size is fixed to the value predicted by the JETSET BEB model tuned at the Z peak, a two-parameter fit to the $D'(Q)$ distribution gives the strength parameter λ consistent with zero:

$$\lambda = -0.004 \pm 0.011 \pm 0.014,$$

which is 4.7σ below the JETSET BEB model prediction of 0.081 ± 0.004 .

Similarly, no enhancement is observed in the $\Delta\rho'$ distribution:

$$I_{\Delta\rho'} = -0.127 \pm 0.143 \pm 0.199.$$

In conclusion, the data are in agreement with the hypothesis where BE correlations are present only for pions coming from the same W. The JETSET model tuned at the Z peak with BE correlations between pions from different W bosons is disfavoured. This statement is in agreement with the previously published ALEPH result on BE correlations in W-pair decays [13] based on the comparison of like-sign and unlike-sign pion pairs. It also agrees with the results from the other LEP experiments [14–16].

Acknowledgments

We are indebted to our colleagues of the accelerator divisions for the outstanding performance of the LEP accelerator. Thanks are also due to the many engineering and technical personnel at CERN and at the home institutes for their contributions toward the success of ALEPH. Those of us from non-member states wish to thank CERN for its hospitality.

References

- [1] G. Goldhaber et al., *Pion-Pion Correlations in Antiproton Annihilation Events*, Phys. Rev. Lett. **3** (1959) 181.
- [2] B. Lorstad, *Boson Interferometry - A Review Of High-Energy Data And Its Interpretation*, Int. J. Mod. Phys. **A4** (1989) 2861; D. H. Boal, C. K. Gelbke, B. K. Jennings, *Intensity Interferometry In Subatomic Physics*, Rev. Mod. Phys. **62** (1990) 553; G. Baym, *The physics of Hanbury Brown-Twiss intensity interferometry: From stars to nuclear collisions*, Acta Phys. Polon. **B29** (1998) 1839; G. Alexander, *Bose-Einstein and Fermi-Dirac interferometry in particle physics*, Rept. Prog. Phys. **66** (2003) 481.
- [3] AFS Collaboration, *Evidence for a Directional Dependence of Bose-Einstein Correlations at the CERN Intersecting Storage Rings*, Phys. Lett. **B187** (1987) 420.
- [4] NA35 Collaboration, *Pion Interferometry with Ultrarelativistic Heavy Ion Collisions from the NA35 Experiment*, Z. Phys **C38** (1988) 79.
- [5] Mark II Collaboration, *Measurement of Energy Correlations in $e^+e^- \rightarrow \text{hadrons}$* , Phys. Rev. Lett. **49** (1982) 521.
- [6] CLEO Collaboration, *Bose-Einstein Correlations in e^+e^- Annihilation in the Υ Region*, Phys. Rev. **D32** (1985) 2294.
- [7] TASSO Collaboration, *Bose-Einstein Correlations Observed in e^+e^- Annihilation at a Center-of-Mass Energy of 34 GeV*, Z. Phys **C30** (1986) 355.
- [8] TPC Collaboration, *Study of Bose-Einstein Correlations in e^+e^- Annihilation at 29 GeV*, Phys. Rev. **D31** (1985) 996.
- [9] ALEPH Collaboration, *A study of Bose-Einstein correlations in e^+e^- annihilations at 91 GeV*, Z. Phys. **C54** (1992) 75; *Two-dimensional analysis of Bose-Einstein correlations in hadronic Z decays at LEP*, Eur. Phys. J. **C36** (2004) 147.
- [10] DELPHI Collaboration, *Bose-Einstein correlations in the hadronic decays of the Z^0* , Phys. Lett. **B286** (1992) 201; *Two-dimensional Analysis of the Bose-Einstein Correlations in e^+e^- Annihilations at the Z peak*, Phys. Lett. **B471** (2000) 460.
- [11] OPAL Collaboration, *A Study of Bose-Einstein Correlations in e^+e^- Annihilations at LEP*, Phys. Lett. **B267** (1991) 143; *Multiplicity dependence of Bose-Einstein correlations in hadronic Z^0 decays*, Z. Phys. **C72** (1996) 389.
- [12] L3 Collaboration, *Bose-Einstein Correlations in the Hadronic Decays of the Z*, Phys. Lett. **B286** (1992) 201; *Measurement of an elongation of the pion source in Z decays*, Phys. Lett. **B458** (1999) 517.
- [13] ALEPH Collaboration, *Bose-Einstein correlations in W-pair decays*, Phys. Lett. **B478** (2000) 50.
- [14] DELPHI Collaboration, *Measurement of correlations between pions from different W's in $e^+e^- \rightarrow W^+W^-$ events*, Phys. Lett. **B401** (1997) 181.

- [15] OPAL Collaboration, *Bose-Einstein Correlations in $e^+e^- \rightarrow W^+W^-$ at 172 and 183 GeV*, Eur. Phys. J. **C8** (1999) 559; *Study of Bose-Einstein Correlations in $e^+e^- \rightarrow W^+W^-$ Events at LEP*, Eur. Phys. J. **C36** (2004) 297.
- [16] L3 Collaboration, *Measurement of Bose-Einstein Correlations in $e^+e^- \rightarrow W^+W^-$ Events at LEP*, Phys. Lett. **B547** (2002) 139.
- [17] L. Lönnblad and T. Sjöstrand, *Bose-Einstein effects and W mass determinations*, Phys. Lett. **B351** (1995) 293.
- [18] S. Jadach and K. Zalewski, *W -mass reconstruction from hadronic events in LEP2: Bose-Einstein effect*, Acta Phys. Pol. **B28** (1997) 1363.
- [19] S.V. Chekanov, E.A. De Wolf and W. Kittel, *Bose-Einstein correlations and color reconnection in W -pair production*, Eur. Phys. J. **C6** (1999) 403.
- [20] ALEPH Collaboration, *ALEPH: a detector for electron-positron annihilations at LEP*, Nucl. Instrum. and Methods **A294** (1990) 121.
- [21] ALEPH Collaboration, *Performance of the ALEPH detector at LEP*, Nucl. Instrum. and Methods **A360** (1995) 481.
- [22] ALEPH Collaboration, *A precise measurement of $\Gamma(Z \rightarrow b\bar{b})/\Gamma(Z \rightarrow \text{hadrons})$* , Phys. Lett. **B313** (1993) 535.
- [23] ALEPH Collaboration, *Measurement of W -pair production in e^+e^- collisions at centre-of-mass energies from 183 to 209 GeV*, CERN preprint CERN-PH-EP-2004-012, submitted to Eur. Phys. J. **C**.
- [24] ALEPH Collaboration, *Measurement of triple gauge-boson couplings at LEP energies up to 189 GeV*, Eur. Phys. J. **C21** (2001) 423.
- [25] L. Lönnblad and T. Sjöstrand, *Modelling Bose-Einstein correlations at LEP2*, Eur. Phys. J. **C2** (1998) 165.
- [26] T. Sjöstrand et al., *High-energy-physics event generation with PYTHIA 6.1*, Comput. Phys. Commun. **135** (2001) 238.
- [27] ALEPH collaboration, *Studies of QCD with the ALEPH detector*, Phys. Rep. **294** (1998) 1.
- [28] ALEPH collaboration, *Study of the fragmentation of b quarks into B mesons at the Z peak*, Phys. Lett. **B512** (2001) 30.
- [29] S. Jadach et al., *The Monte Carlo program KoralW version 1.51 and the concurrent Monte Carlo KoralW&YFSWW3 with all background graphs and first-order corrections to W -pair production*, Comput. Phys. Commun. **140** (2001) 475.
- [30] S. Jadach, B.F.L. Ward and Z. Wąs, *The precision Monte Carlo event generator KK for two-fermion final states in e^+e^- collisions*, Comput. Phys. Commun. **130** (2000) 260.

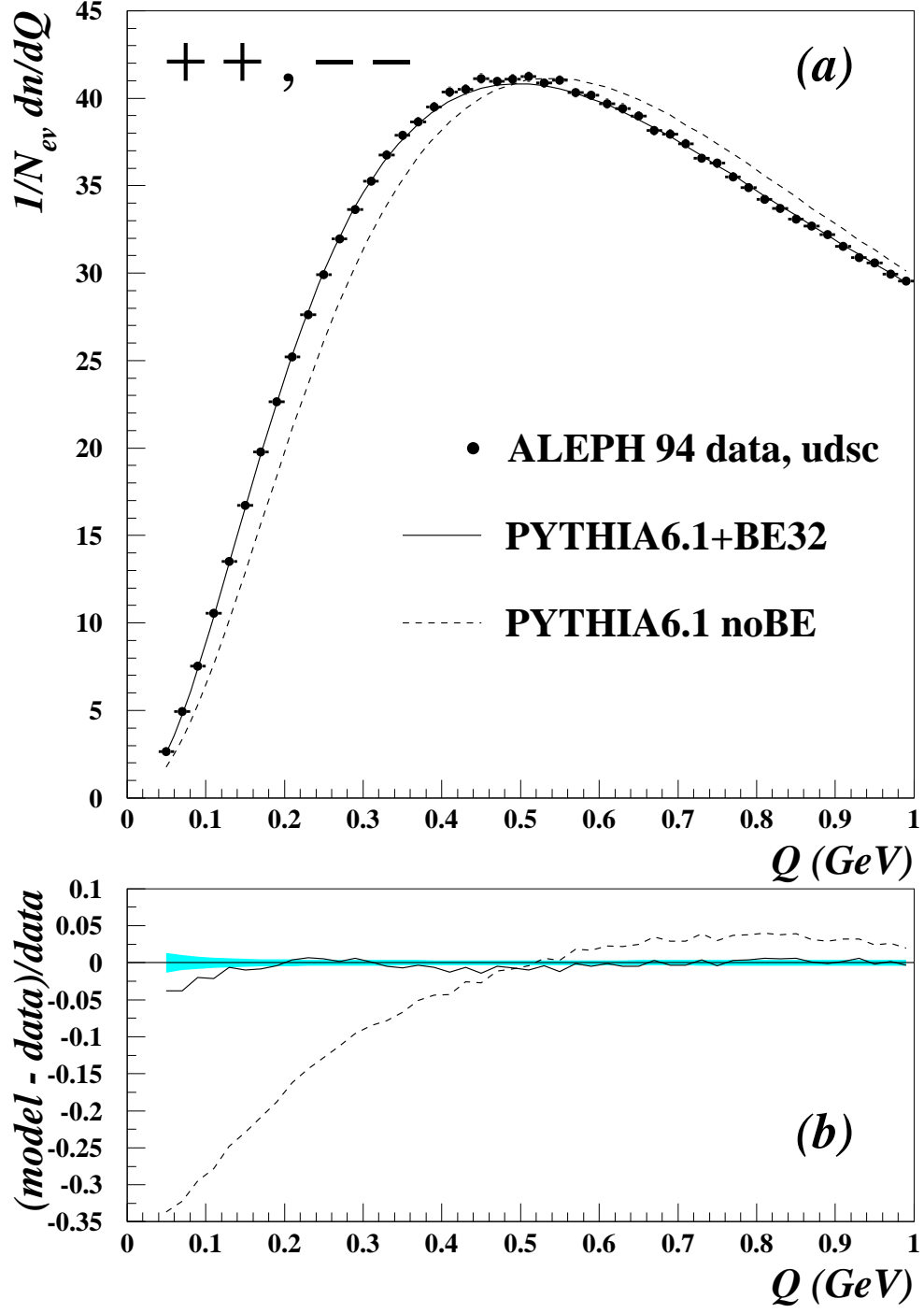


Figure 1: The normalized and corrected Q distribution of same-sign charged particle pairs in b -depleted Z decays, compared to model predictions (a). The relative deviation of the model predictions from the data is shown in (b). The grey band indicates the statistical errors.

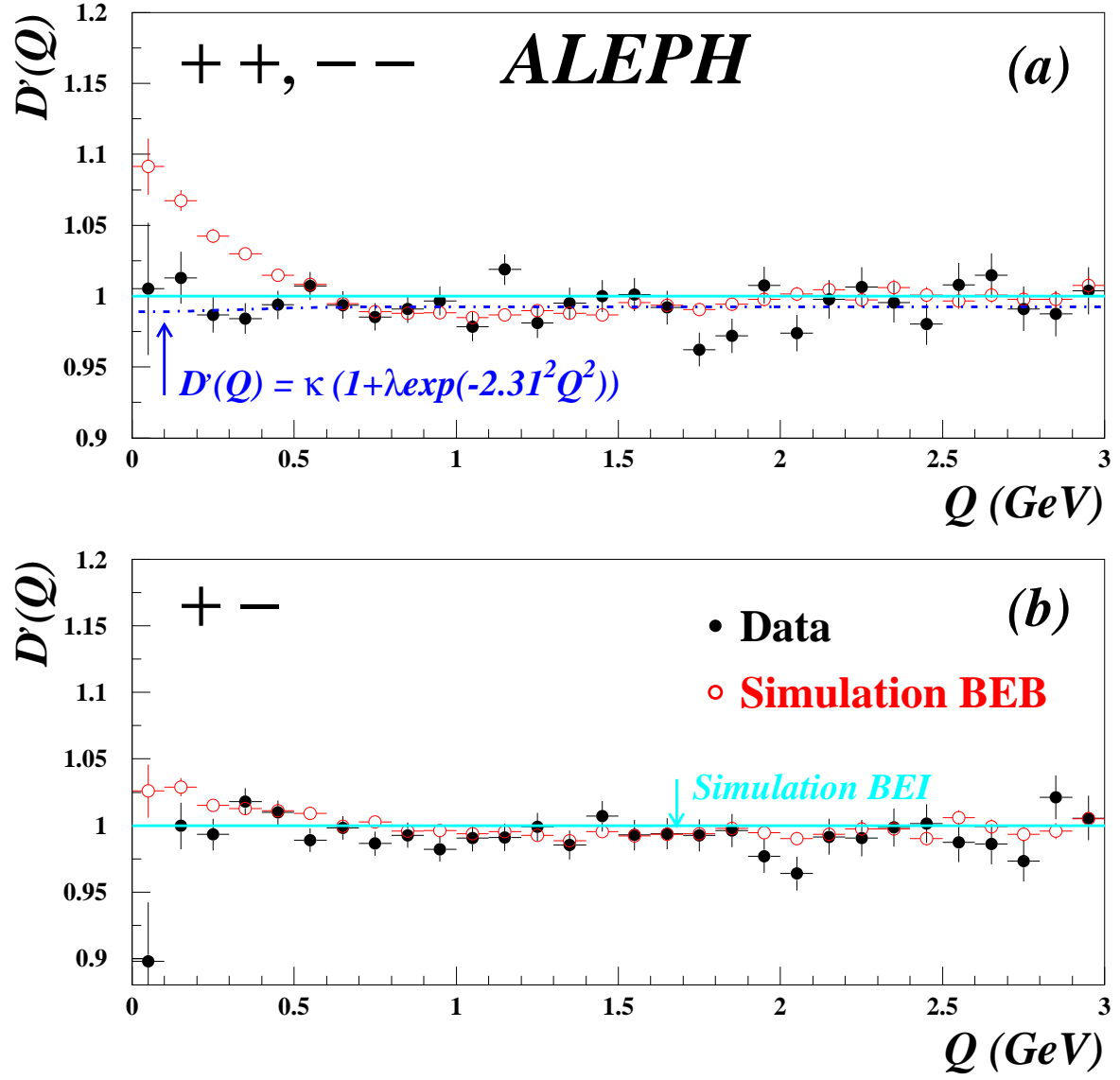


Figure 2: $D'(Q)$ distributions for data and simulation with Bose-Einstein correlations for like-sign pairs (a) and unlike-sign pairs (b). Only statistical uncertainties are shown. The dashed-dotted line represents the results of the two-parameter fit to the data.

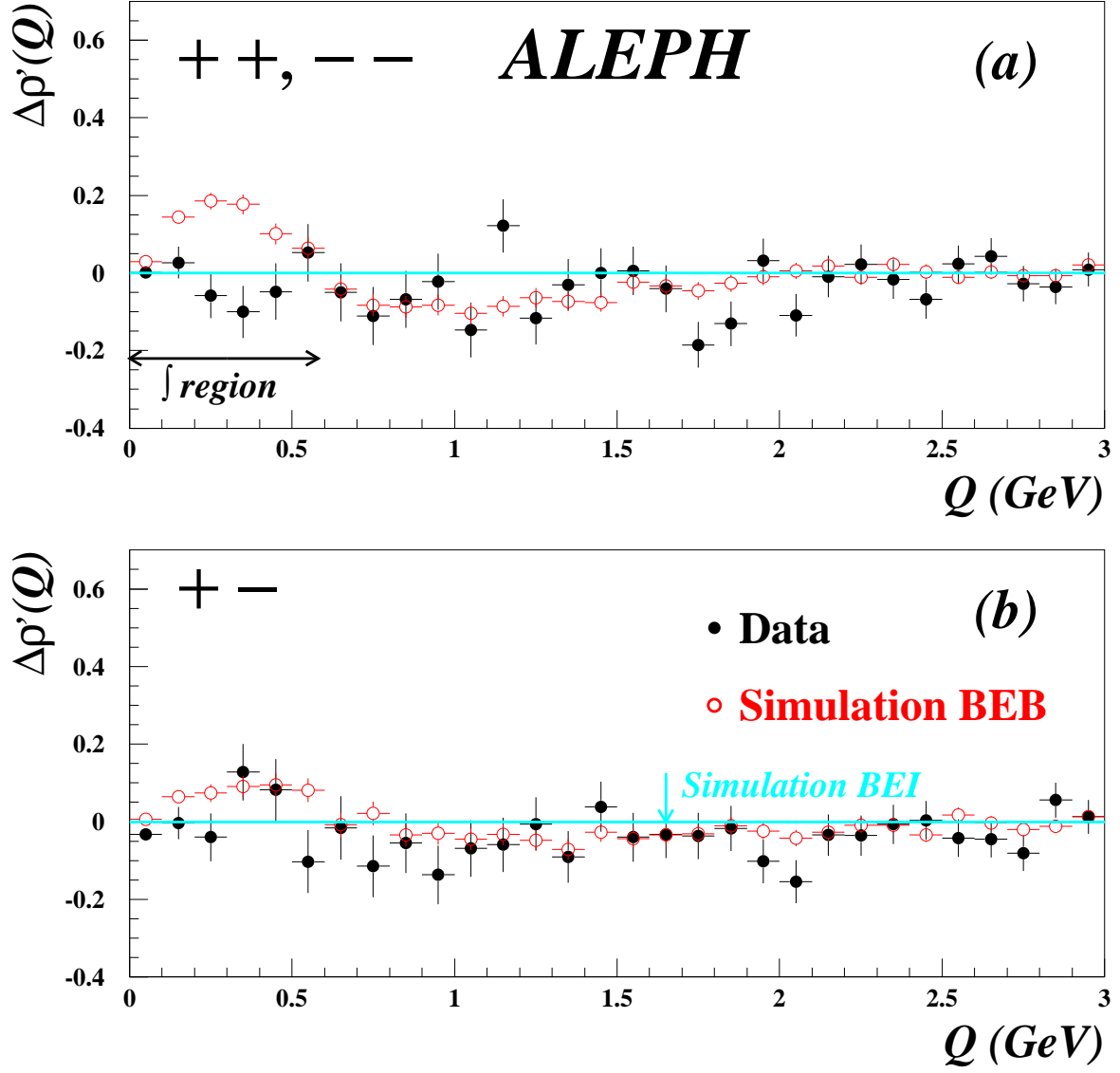


Figure 3: $\Delta\rho'(Q)$ distributions for data and simulation with Bose-Einstein correlations for like-sign pairs (a) and unlike-sign pairs (b). Only statistical uncertainties are shown.